

A phenomenological theory of zero-energy Andreev resonant states

Yasuhiro Asano*

Department of Applied Physics, Hokkaido University, Sapporo 060-8628, Japan

Yukio Tanaka

Department of Applied Physics, Nagoya University, Nagoya 464-8603, Japan

Satoshi Kashiwaya

National Institute of Advanced Industrial Science and Technology, Tsukuba, 305-8568, Japan

(Dated: May 22, 2019)

A conceptual consideration is given to a zero-energy state (ZES) at the surface of unconventional superconductors. The reflection coefficients in normal-metal / superconductor (NS) junctions are calculated based on a phenomenological description of the reflection processes of a quasiparticle. The phenomenological theory reveals the importance of the sign change in the pair potential for the formation of the ZES. The ZES is observed as the zero-bias conductance peak (ZBCP) in the differential conductance of NS junctions. The split of the ZBCP due to broken time-reversal symmetry states is naturally understood in the present theory. We also discuss effects of external magnetic fields on the ZBCP.

PACS numbers: 74.50.+r, 74.25.Fy, 74.70.Tx

I. INTRODUCTION

Transport phenomena in unconventional superconductors have attracted considerable interest in recent years because high- T_c superconductors may have the d wave pairing symmetry^{1,2,3}. The unconventional pairing symmetry causes the anisotropy in transport properties such as the electric conductance and the thermal conductivity^{4,5}. In normal-metal / high- T_c superconductor junctions, for instance, the shape of the differential conductance reflects the density of states when the a axis of high- T_c materials is perpendicular to the junction interface. When a axis deviates from the interface normal, on the other hand, the conductance shows a large peak at the zero bias-voltage^{6,7,8,9,10,11,12,13,14,15,16,17,18}. Such anisotropy in the conductance is now explained by the formation of a zero-energy state (ZES)^{6,19} at the interface of junctions. Since the ZES appears just on the Fermi energy, it drastically affects transport properties through the interface of unconventional superconductor junctions. The low-temperature anomaly of the Josephson current between the two unconventional superconductors is explained in terms of the resonant tunneling of Cooper pairs via the ZES^{20,21,22,23,24}. So far a considerable number of studies have been made on the ZES itself and related phenomena of transport properties in both spin-singlet and spin-triplet unconventional superconductor junctions^{7,8,25,26,27,28,29,30,31,32,33,34,35,36,37,38,39,40,41,42,43,44,45,46,47,48,49,50}.

The conductance in normal-metal / superconductor (NS) junctions is calculated from the normal and the Andreev reflection⁵¹ coefficients which are obtained by solving the Bogoliubov-de Gennes (BdG) equation⁵² under appropriate boundary conditions at the junction interface. Consequently we easily find the zero-bias conductance peak (ZBCP) in NS junctions of high- T_c supercon-

ductors⁶. Although the algebra itself is straightforward, it is not easy to understand the physics behind the calculation. In a previous paper⁵³, we briefly discussed reasons for the appearance of the ZBCP by a phenomenological argument. The phenomenological analysis has several advantages. For instance, it shows the importance of the unconventional pairing symmetry for the formation of the ZES without directly solving the BdG equation. Moreover we easily understand that the ZES is a result of the interference effect of a quasiparticle. The applicability of the analysis in the previous paper, however, is very limited because of its simplicity.

In this paper, we reconstruct the phenomenological theory of the Andreev reflection to meet the mathematical accuracy. We calculate the reflection coefficients of an electronlike quasiparticle incident from a normal metal into a NS interface. Near the junction interface, a quasiparticle suffers two kinds of reflection: (i) the normal reflection by the barrier potential at the NS interface and (ii) the Andreev reflection by the pair potential in the superconductor. In the present theory, we consider the two reflections separately to calculate the transport coefficients. As a consequence, the Andreev reflection coefficient is decomposed into a series expansion with respect to the normal reflection probability of NS junctions. The expression of the Andreev reflection probability enables us to understand the importance of the unconventional pairing symmetry for the formation of the ZES. In unconventional superconductors, the pair potential in the electron branch (Δ_+) differs from that in the hole branch (Δ_-). The Andreev reflection probability at the zero-energy is expressed as the summation of the alternating series when Δ_+ and Δ_- have the same sign. In this case, the zero-bias conductance becomes a small value proportional to $|t_N|^4$, where $|t_N|^2$ is the normal transmission probability of junctions. On the other

hand when $\Delta_+ \Delta_- < 0$, all the expansion series have the same sign and the conductance has a large peak at the zero-bias. The phenomenological theory can be applied to superconductors with a broken time-reversal symmetry state (BTRSS)^{54,55,56,57,58,59,60,61,62,63,64,65,66,67} and NS junctions under external magnetic fields^{54,68,69,70}.

This paper is organized as follows. In Sec. II, the Andreev and the normal reflection coefficients are derived from a phenomenological description of a quasiparticle's motion near the NS interface. In Sec. III, we discuss the conductance peaks in NS junctions. A relation between the broken time-reversal symmetry states and the peak position in the conductance is discussed in Sec. IV. We apply the phenomenological theory to NS junctions under magnetic fields in Sec. V. In Sec. IV, we summarize this paper.

II. QUASIPARTICLE'S MOTION NEAR NS INTERFACES

Let us consider two-dimensional NS junctions as shown in Fig. 1, where a normal-metal ($x < 0$) and a superconductor ($x > 0$) are separated by a potential barrier $V(\mathbf{r}) = V_b \delta(x)$. We assume the periodic boundary condition in the y direction and the width of the junction is W . The NS junctions are described by the Bogoliubov-de Gennes equation⁵²,

$$\int d\mathbf{r}' \begin{pmatrix} \delta(\mathbf{r} - \mathbf{r}') h_0(\mathbf{r}') & \Delta(\mathbf{r}, \mathbf{r}') e^{i\varphi_s} \\ \Delta^*(\mathbf{r}, \mathbf{r}') e^{-i\varphi_s} & -\delta(\mathbf{r} - \mathbf{r}') h_0(\mathbf{r}') \end{pmatrix} \times \begin{pmatrix} u(\mathbf{r}') \\ v(\mathbf{r}') \end{pmatrix} = E \begin{pmatrix} u(\mathbf{r}) \\ v(\mathbf{r}) \end{pmatrix}, \quad (1)$$

$$h_0(\mathbf{r}) = -\frac{\hbar^2 \nabla^2}{2m} + V_b \delta(x) - \mu_F, \quad (2)$$

$$\Delta(\mathbf{R}_c, \mathbf{r}_r) = \begin{cases} \frac{1}{V_{vol}} \sum_{\mathbf{k}} \Delta(\mathbf{k}) e^{i\mathbf{k} \cdot \mathbf{r}_r} & : X_c > 0 \\ 0 & : X_c < 0 \end{cases}, \quad (3)$$

where φ_s is a macroscopic phase of the superconductor, $\mathbf{R}_c = (X_c, Y_c) = (\mathbf{r} + \mathbf{r}')/2$ and $\mathbf{r}_r = \mathbf{r} - \mathbf{r}'$. Here we assume spin-singlet superconductors for simplicity. The argument in the following can be extended to spin-triplet superconductors as shown in Appendix. When an electronlike quasiparticle is incident from the normal metal as shown in Fig. 1, the wave function in the normal metal is given by,

$$\Psi_N(\mathbf{r}) = \left[\begin{pmatrix} 1 \\ 0 \end{pmatrix} e^{ik_x x} + \begin{pmatrix} 1 \\ 0 \end{pmatrix} e^{-ik_x x} \right] e^{ik_y y} + \begin{pmatrix} 0 \\ 1 \end{pmatrix} e^{ik_x x} e^{ik_y y} \frac{e^{i\varphi_s}}{\sqrt{W}}. \quad (4)$$

where k_x and k_y are the wave numbers on the Fermi surface. They satisfy $k_x^2 + k_y^2 = k_F^2$, where k_F is the Fermi wave number. Throughout this paper we assume that $E \sim \Delta_0 \ll \mu_F$, where Δ_0 is the amplitude of the pair

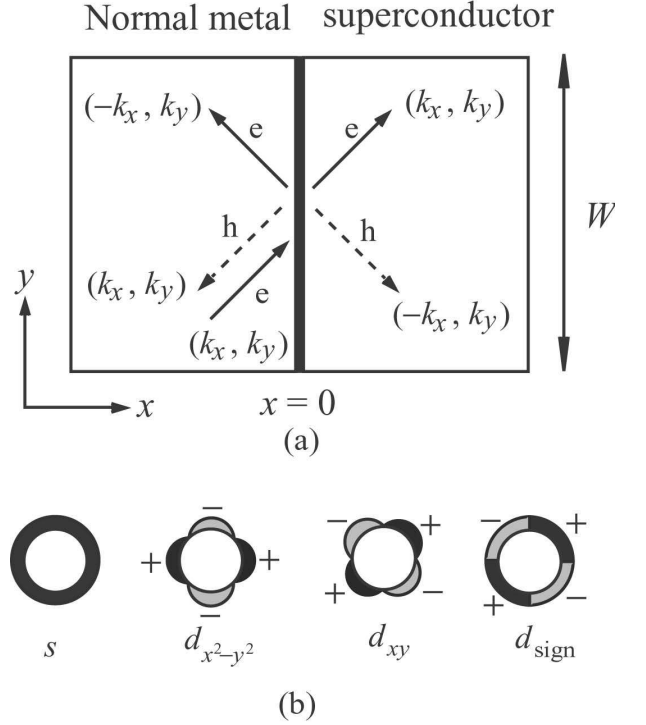


FIG. 1: A normal-metal / superconductor junction is illustrated in (a). When an electronlike quasiparticle is incident from the normal metal, directions of the outgoing waves are indicated by arrows. The trajectories of a quasiparticle in the electron branch and those in the hole branch are denoted by solid and broken lines, respectively. In (b), the pair potentials of s , $d_{x^2-y^2}$ and d_{xy} wave symmetries are schematically illustrated.

potential and E is the energy of a quasiparticle measured from the Fermi energy, $\mu_F = \hbar^2 k_F^2 / (2m)$.

When a quasiparticle is incident from the normal metal in the electron branch, directions of the outgoing waves are indicated by arrows as shown in Fig. 1. The trajectories of a quasiparticle in the electron branch and those in the hole branches are denoted by solid and broken lines, respectively. In the normal metal, a velocity component perpendicular to the interface changes its sign in the normal reflection, whereas all velocity components change signs in the Andreev reflection. In the superconductor, the wave number in the electron branch is (k_x, k_y) , but that in the hole branch becomes $(-k_x, k_y)$. In unconventional superconductors, the pair potential in the electron branch ($\Delta_+ \equiv \Delta(k_x, k_y)$) differs from that in the hole branch ($\Delta_- \equiv \Delta(-k_x, k_y)$). Therefore the wave function in the superconductor is described by these two pair

potentials,

$$\Psi_S(\mathbf{r}) = \left[\begin{pmatrix} u_+ \\ e^{-i\phi_+} e^{-i\varphi} v_+ \end{pmatrix} e^{ik^e_x t^e} + \begin{pmatrix} e^{i\phi_-} e^{i\varphi} v_- \\ u_- \end{pmatrix} e^{-ik^h_x t^h} \right] \frac{e^{ik_y y}}{\sqrt{W}}, \quad (5)$$

$$u_{\pm}(v_{\pm}) = \sqrt{\frac{1}{2} \left(1 + (-) \frac{\Omega_{\pm}}{E} \right)}, \quad (6)$$

$$e^{i\phi_{\pm}} \equiv \frac{\Delta_{\pm}}{|\Delta_{\pm}|}, \quad (7)$$

$$k^{e(h)} = \left[k_x^2 + (-) k_F^2 \frac{\sqrt{E^2 - |\Delta_{+(-)}|^2}}{\mu_F} \right]^{1/2}, \quad (8)$$

$$\Omega_{\pm} = \sqrt{E^2 - |\Delta_{\pm}|^2}. \quad (9)$$

The wave numbers of a quasiparticle are approximately given by $k^{e(h)} \approx k_x + (-)i/(2\xi_0)$ for $E \sim 0$, where $\xi_0 = \hbar v_F/(\pi\Delta_0)$ is the coherence length and v_F is the Fermi velocity. Thus a quasiparticle penetrates into the superconductor within a range of ξ_0 . In Eqs. (5)-(7), a phase $e^{i\phi_{\pm}}$ represents the sign of the pair potential and appears in the wave function in addition to a macroscopic phase of the superconductor. The transmission and the reflection coefficients are obtained from the boundary conditions of these wave functions. Near the junction interface, an incident quasiparticle suffers two kinds of reflection: (i) the normal reflection by the barrier potential at the NS interface and (ii) the Andreev reflection by the pair potential in the superconductor. In this paper, we consider contributions of the two reflection processes to the reflection coefficients separately.

We first consider NS junctions with no barrier potential at the interface,

$$z_0 \equiv \frac{V_b}{v_F} = 0, \quad (10)$$

where z_0 represents the strength of the potential barrier. The Andreev reflection coefficients become

$$r_0^{he} = -i\nu_+ e^{-i\phi_+} e^{-i\varphi}, \quad (11)$$

$$r_0^{eh} = -i\nu_- e^{i\phi_-} e^{i\varphi}, \quad (12)$$

$$\nu_{\pm} = i \frac{E - \Omega_{\pm}}{|\Delta_{\pm}|}, \quad (13)$$

where r_0^{he} is the Andreev reflection coefficients from the electron branch to the hole branch in the absence of the potential barrier. We also give the Andreev reflection coefficient from the hole branch to the electron branch (r_0^{eh}). In the case of $E^2 - \Delta_{\pm}^2 < 0$, ν_{\pm} can be described as

$$\nu_{\pm} = \frac{\sqrt{\Delta_{\pm}^2 - E^2}}{|\Delta_{\pm}|} + i \frac{E}{|\Delta_{\pm}|}, \quad (14)$$

$$\equiv \cos \theta_{\pm} + i \sin \theta_{\pm} = e^{i\theta_{\pm}}. \quad (15)$$

Thus the Andreev reflection coefficients include only the phase information in the limit of $z_0 = 0$.

We next consider the reflection by the potential barrier in a phenomenological way. In the presence of the potential barrier, the Andreev reflection processes are shown in Fig. 2. In the electron branch, the nor-

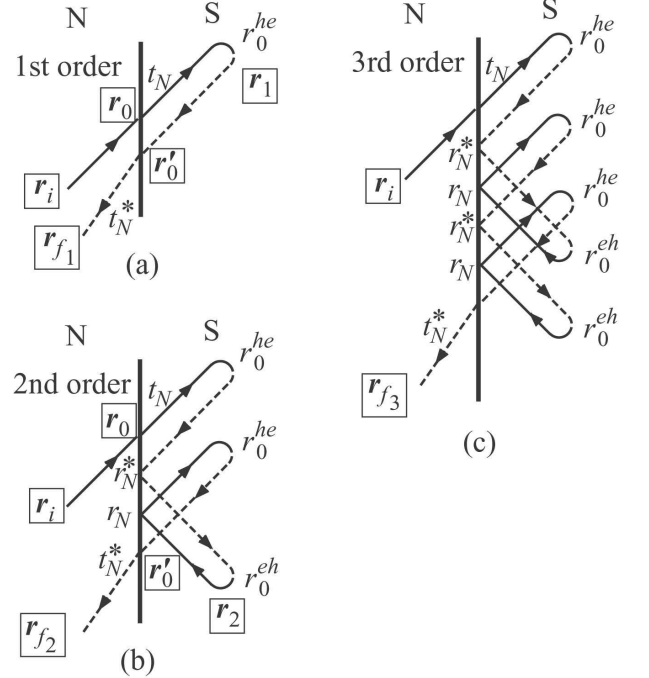


FIG. 2: The Andreev reflection processes are decomposed into a series of the reflections by the pair potential and the barrier potential.

mal transmission and the normal reflection coefficients of the barrier are calculated to be $t_N = \bar{k}_x/(\bar{k}_x + iz_0)$ and $r_N = -iz_0/(\bar{k}_x + iz_0)$, respectively with $k_x = k_x/k_F$. Those in the hole branch are t_N^* and r_N^* . The Andreev reflection coefficient in the 1st order process is given by,

$$r^{he}(1) = t_N^* \cdot r_0^{he} \cdot t_N. \quad (16)$$

At first an electronlike quasiparticle starting from \mathbf{r}_i transmits into the superconductor through \mathbf{r}_0 (t_N). In Fig. 2, the vectors in real space are surrounded by squares to avoid confusion. While traveling the superconductor within the range of ξ_0 , the quasiparticle is reflected into the hole branch by the pair potential at \mathbf{r}_1 (r_0^{he}). Then the quasiparticle goes back to the normal metal in the hole branch through \mathbf{r}'_0 (t_N^*). The 2nd order Andreev reflection process in Fig. 2 (b) can be estimated in the same way,

$$r^{he}(2) = t_N^* \cdot A_S \cdot r_0^{he} \cdot t_N, \quad (17)$$

$$A_S = r_0^{he} \cdot r_N \cdot r_0^{eh} \cdot r_N^*, \quad (18)$$

$$= -|r_N|^2 \nu_+ \nu_- e^{i(\phi_- - \phi_+)}, \quad (19)$$

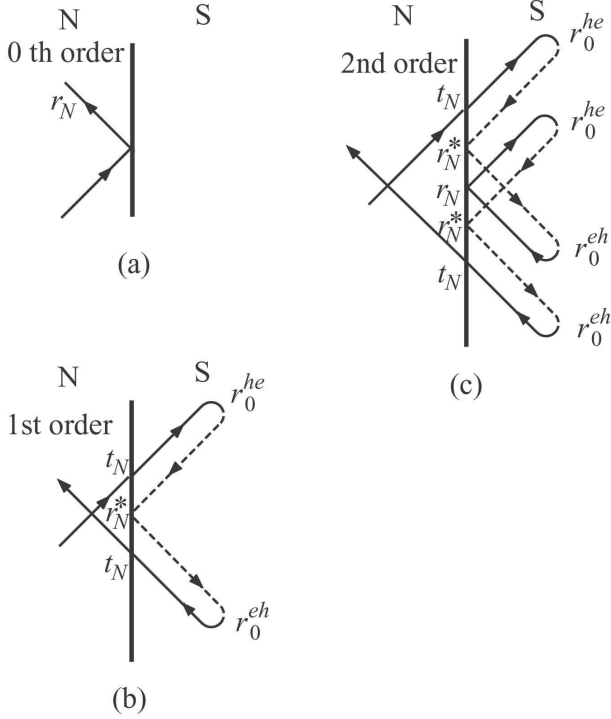


FIG. 3: The normal reflection processes are decomposed into a series of the reflections by the pair potential and the barrier potential.

After the first Andreev reflection into the hole branch, the quasiparticle suffers the normal reflection (r_N^*). Next the holelike quasiparticle experiences the 2nd Andreev reflection to the electron branch at \mathbf{r}_2 (r_0^{eh}). Then the electronlike quasiparticle suffers the normal reflection (r_N) followed by the 3rd Andreev reflection into the hole branch (r_0^{he}). Finally the holelike quasiparticle goes back to the normal metal through \mathbf{r}_0' (t_N^*). We only show the expression of the Andreev reflection coefficient in the 3rd order process,

$$r^{he}(3) = t_N^* \cdot A_S^2 \cdot r_0^{he} \cdot t_N. \quad (20)$$

The corresponding trajectory is shown in Fig. 2 (c). The total Andreev reflection coefficient is obtained by the summation of these reflection processes up to the infinite order,

$$r^{he} = |t_N|^2 \cdot r_0^{he} \cdot \sum_{n=1}^{\infty} A_S^{n-1} \quad (21)$$

$$= \frac{|t_N|^2 r_0^{he}}{1 - |r_N|^2 r_0^{he} r_0^{eh}}. \quad (22)$$

In the similar way, the normal reflection coefficient results

in

$$r^{ee} = r_N + t_N^2 \cdot r_N^* \cdot r_0^{he} r_0^{eh} \sum_{n=1}^{\infty} A_S^{n-1}, \quad (23)$$

$$= r_N \frac{r_0^{he} r_0^{eh}}{1 - |r_N|^2 r_0^{he} r_0^{eh}}. \quad (24)$$

The corresponding trajectories for the normal reflection are shown in Fig. 3. Although the reflection coefficients in Eqs. (22) and (24) are obtained based on the phenomenological description of a quasiparticle's motion, they are mathematically identical to the exact expressions calculated from the boundary conditions of the wave functions in the presence of the potential barrier⁶.

III. CONDUCTANCE

The differential conductance is calculated from the normal and the Andreev reflection coefficients^{71,72},

$$G_{NS} = \frac{2e^2}{h} \sum_{k_y} [1 - |r^{ee}|^2 + |r^{he}|^2] \Big|_{E=eV_{bias}}, \quad (25)$$

where V_{bias} is the bias voltage applied to NS junctions. We focus on the limit of $E \rightarrow 0$ for a while, where the Andreev reflection probability dominates the zero-bias conductance because the conductance can be described by

$$G_{NS} = \frac{4e^2}{h} \sum_{k_y} |r^{he}|^2 \Big|_{E=eV_{bias}}. \quad (26)$$

A quasiparticle after the Andreev reflection traces back the original trajectory of a quasiparticle before the Andreev reflection. This is called the retro property of a quasiparticle. When we estimate the reflection coefficients in Eq. (21) and (23), we only consider the phase factor of the Andreev reflection. A quasiparticle, however, may suffer additional phase shift while moving around the NS interface. Actually, an electron acquires a phase $e^{i\mathbf{k} \cdot (\mathbf{r}_1 - \mathbf{r}_0)}$ while traveling from \mathbf{r}_0 to \mathbf{r}_1 as shown in Fig. 2 (a). In addition to this, a phase factor $e^{i\mathbf{k} \cdot (\mathbf{r}_0' - \mathbf{r}_1)}$ is multiplied while traveling from \mathbf{r}_1 to \mathbf{r}_0' in the hole branch. These two phase factors exactly cancel each other out when the retro property holds because $\mathbf{r}_0 = \mathbf{r}_0'$. Thus \mathbf{r}_{f_n} indicates the same position for all n . In particular for $E = 0$, a relation $\mathbf{r}_i = \mathbf{r}_{f_n}$ for all n holds, which means the retro property of a quasiparticle in the normal metal. In the limit of $E \rightarrow 0$, we find in Eq. (15) that $\nu_{\pm} \rightarrow 1$ irrespective of the symmetry of the pair potential. The Andreev reflection probability becomes

$$|r^{he}|^2 = |t_N|^4 \left| \sum_{n=0}^{\infty} |r_N|^{2n} [-e^{i(\phi_- - \phi_+)}]^n \right|^2, \quad (27)$$

$$= \frac{|t_N|^4}{|1 + |r_N|^2 e^{i(\phi_- - \phi_+)}|^2}. \quad (28)$$

Firstly, we consider superconductors where the pair potentials in the two branches (Δ_+ and Δ_-) have the same sign, (i.e., $e^{i(\phi_- - \phi_+)} = 1$). For examples, the pair potentials below satisfy the condition irrespective of the wave numbers of a quasiparticle,

$$\Delta_s = \Delta_0 \quad (s \text{ wave}), \quad (29)$$

$$\Delta_{d_{x^2-y^2}}(\mathbf{k}) = \Delta_0(\bar{k}_x^2 - \bar{k}_y^2) \quad (d_{x^2-y^2} \text{ wave}), \quad (30)$$

where $\bar{k}_x = k_x/k_F$ and $\bar{k}_y = k_y/k_F$ are the normalized wave number on the Fermi surface in the x and y directions, respectively. The schematic figures of the pair potentials are shown in Fig. 1 (b). Equation (29) represents the pair potential of s wave superconductors. The pair potential in Eq. (30) is realized in a junction where the a axis of a high- T_c superconductor is perpendicular to the interface normal. When $e^{i(\phi_- - \phi_+)} = 1$ is satisfied, Eq. (27) becomes the summation of the alternating series. The Andreev reflection probability results in

$$|r^{he}|^2 = \frac{2|t_N|^4}{(2 - |t_N|^2)^2}. \quad (31)$$

In low transparent junctions, (i.e., $z_0^2 \gg 1$), the Andreev reflection probability is a small value $|t_N|^4/2 \propto 1/z_0^4$. Therefore the zero-bias conductance in Eq.(26) is proportional to $1/z_0^4$. Secondly we consider that the signs of the two pair potential are opposite to each other. The pair potential

$$\Delta_{d_{xy}}(\mathbf{k}) = 2\Delta_0\bar{k}_x\bar{k}_y, \quad (d_{xy} \text{ wave}), \quad (32)$$

satisfies $e^{i(\phi_- - \phi_+)} = -1$ for all wave numbers and is realized in a junction where the a axis of a high- T_c superconductor is oriented by 45 degree from the interface normal. All the expansion series in Eq. (27) have the same sign and the Andreev reflection probability becomes

$$|r^{he}|^2 = 1. \quad (33)$$

Thus the zero-bias conductance in Eq.(26) takes its maximum value. The sign of the pair potentials characterizes the interference effect of a quasiparticle near the NS interface. For $e^{i(\phi_- - \phi_+)} = 1$, the alternating series in Eq. (27) reflect the destructive interference among the partial waves of a quasiparticle in the expansion series. Hence the conductance becomes small at the zero-bias. On the other hand for $e^{i(\phi_- - \phi_+)} = -1$, the expansion series with the same sign imply that the partial waves in the expansion series interfere constructively, which leads to the large zero-bias conductance. The constructive interference at the interface causes a resonant state which is now referred to as the ZES. The Andreev reflection probability is unity independent of the normal transmission probability of junctions as shown in Eq. (33). This can be interpreted as a result of the resonant transmission of a quasiparticle through the ZES. A microscopic calculation shows that the ZES has a large local density of states around $x = \xi_0$ at the zero-energy⁷³.

In Eq. (33), we can explain a large conductance at the zero-bias. In what follows, we will show that the conductance has a peak structure around the zero-bias. When $E \neq 0$ but still $E \ll \Delta_0$, the degree of resonance is suppressed because ν_{\pm} is no longer unity as shown in Eq. (15). In the superconductor, the argument of the phase cancellation in the round-trip between \mathbf{r}_0 and \mathbf{r}_1 in Fig. 2 (a) is still valid as far as $E^2 - |\Delta_{\pm}|^2 < 0$ is satisfied. In the electron branch on the way to \mathbf{r}_1 , the x component of the wavenumber is given by

$$k^e \simeq k_x + i \frac{k_F}{k_x} \frac{\sqrt{|\Delta_+|^2 - E^2}}{2\mu_F}, \quad (34)$$

The real part determines the direction of the quasiparticle's motion. The inverse of the imaginary part characterizes the dumping of the wave function and is roughly estimated to be ξ_0 . It is also shown that k_x is the real part of the wave number in the hole branch on the way back to \mathbf{r}_0 . The Andreev reflection probability for finite E is given by

$$|r^{he}|^2 = \frac{|t_N|^4}{|t_N|^4 + 2|r_N|^2(1 + \text{Re}\nu_+\nu_-e^{i(\phi_- - \phi_+)})}. \quad (35)$$

To make clear a relation between the peak positions of the conductance and the relative sign of the pair potentials, we consider the pair potential

$$\Delta_{d_{\text{sign}}}(\mathbf{k}) = \Delta_0 \text{sgn}(k_x k_y). \quad (36)$$

instead of Eq.(32). Here the anisotropy of pair potential is taken into account only through the phase $e^{i\phi_{\pm}}$ and the \mathbf{k} dependence of the pair potential is neglected. The pair potential in Eq. (36) is illustrated in Fig. 1 (b). We will check the validity of Eq. (36) later. The Andreev reflection probability for $\Delta_{d_{\text{sign}}}$ becomes

$$|r^{he}|^2 = \frac{|t_N|^4}{|t_N|^4 + 4|r_N|^2 \sin^2 \theta}, \quad (37)$$

$$= \frac{E_0^2}{E^2 + E_0^2}, \quad (38)$$

$$E_0 = \frac{\Delta_0 |t_N|^2}{2|r_N|}. \quad (39)$$

where we use a relation $\theta = \theta_+ = \theta_-$ and $\sin \theta = E/\Delta_0$ in Eq. (15). The Andreev reflection probability has a peak structure at $E = 0$ and the width of the peak is characterized by E_0 which is Δ_0/z_0^2 in the limit of $z_0^2 \gg 1$. On the other hand in s wave junctions (i.e., $e^{i(\phi_- - \phi_+)} = 1$), we find

$$|r^{he}|^2 = \frac{|t_N|^4}{|t_N|^4 + 4|r_N|^2 \cos^2 \theta}, \quad (40)$$

$$= \frac{E_0^2}{(\Delta_0^2 - E^2) + E_0^2}, \quad (41)$$

where $\cos \theta = \sqrt{\Delta_0^2 - E^2}/\Delta_0$ in Eq. (15). The Andreev reflection probability has a peak at $E = \Delta_0$ reflecting

a peak of the bulk density of states in s wave superconductors. Above analysis implies that the peak position is determined by $\sin \theta = 0$ for $e^{i(\phi_- - \phi_+)} = -1$ and $\cos \theta = 0$ for $e^{i(\phi_- - \phi_+)} = 1$. In Fig. 4, we plot the conductance, where $z_0 = 3$ and $N_c = Wk_F/\pi$ is the number of propagating channels on the Fermi surface. The results for s wave junction are indicated by the bro-

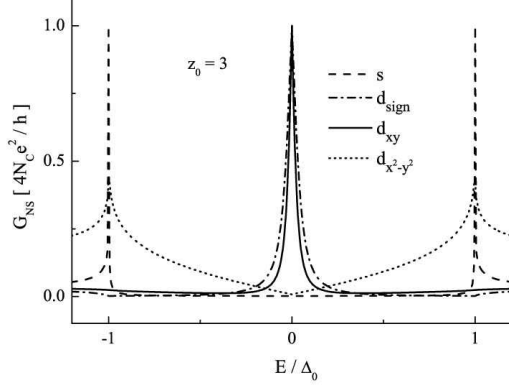


FIG. 4: The conductance is plotted as a function of E , where $z_0 = 3$. The anisotropy of the pair potential in d_{xy} symmetry is taken into account only through the phase factor $e^{i(\phi_- - \phi_+)}$ and \mathbf{k} dependence of the pair potential is neglected in the dash-dotted line. The d_{xy} symmetry is fully taken into account in the solid line. The conductance for $d_{x^2-y^2}$ symmetry is amplified by 5 times in the dotted line.

ken line, where the subgap conductance is exactly given by Eqs. (40) and (26). The conductance has a peak at $E = \Delta_0$. The conductance for $d_{x^2-y^2}$ symmetry is amplified by 5 times in the dotted line and also has a peak at $E = \Delta_0$ corresponding to the bulk density of states. The results for $\Delta_{d_{\text{sign}}}$ are shown with the dash-dotted line, where the subgap conductance is calculated from Eqs. (37) and (26). We also show the conductance of d_{xy} wave junctions with the solid line, where the conductance is calculated from the normal and the Andreev reflection coefficients based on Eq. (25). There is no significant difference between the conductance for d_{xy} symmetry and that for d_{sign} in Eq. (36) because the relative sign of the two pair potential ($e^{i(\phi_- - \phi_+)} = -1$) dominates the subgap conductance structure. Throughout this paper, we describe the pair potential by using the step function at the NS interface and neglect its spatial dependence in superconductors. In real NS junctions, the pair potential is suppressed at the interface in the presence of the ZES^{60,65}. The conductance shape around the zero-bias, however, almost remains unchanged even if the spatial dependence of the pair potential is taken into account⁷⁴. This is also because relative sign of the two pair potentials determines the conductance around the zero-bias. The spatial dependence of the pair potential may affect

the width of the ZBCP through E_0 in Eq.(39).

We note that there is no remarkable differences between the mathematical origin of the peaks at $E = 0$ for $e^{i(\phi_- - \phi_+)} = -1$ and that $E = \Delta_0$ for $e^{i(\phi_- - \phi_+)} = 1$. Actually it is easy to confirm at $E = \Delta_0$ that the Andreev reflection probability in s wave junctions becomes

$$|r^{he}|^2 = |t_N|^4 \left| \sum_{n=0}^{\infty} |r_N|^{2n} \left[e^{i(\phi_- - \phi_+)} \right]^n \right|^2. \quad (42)$$

All the expansion series have the same sign for $e^{i(\phi_- - \phi_+)} = 1$. Thus we may say that the peak position of the conductance represents the energy of resonant states in superconductors.

IV. PAIRING WITHOUT TIME-REVERSAL SYMMETRY

In recent experiments, a possibility of the broken time reversal symmetry state (BTRSS) at the surface of high- T_c superconductors has been discussed^{55,56,57,58,59}. These experiments found the split of the ZBCP in the zero magnetic field. It is pointed out that such surface states may have $s + id_{xy}$ ⁶⁰ or $d_{xy} + id_{x^2-y^2}$ ⁶¹ pairing symmetry. Theoretical studies showed the split of the surface density of states^{54,62,63,64,65,66} when $s + id_{xy}$ wave pairing symmetry is assumed at the surface of the d_{xy} superconductor. Within the present phenomenological theory, it is also possible to discuss the split of the conductance peak by the BTRSS. We assume the pair potential as

$$\Delta_{s+id_{xy}}(\mathbf{k}) = \alpha \Delta_0 + i\beta \Delta_{d_{xy}}(\mathbf{k}), \quad (s + id_{xy} \text{ wave}), \quad (43)$$

with $\alpha^2 + \beta^2 = 1$. We find

$$|\Delta_{\pm}| = |\Delta| = \sqrt{\alpha^2 \Delta_0^2 + \beta^2 \Delta_{d_{xy}}^2(\mathbf{k})}, \quad (44)$$

$$e^{i(\phi_- - \phi_+)} = e^{2i\phi_-} = \left[\frac{\alpha \Delta_0 - i\beta \Delta_{d_{xy}}}{|\Delta|} \right]^2. \quad (45)$$

In Fig 5, we show the conductance in the $s + id_{xy}$ symmetry for several α . For $\alpha = 0$, the results are identical to the conductance of d_{xy} wave junctions in Fig. 4. The ZBCP splits into two peaks for $\alpha \neq 0$. The splitting width increases almost linearly with increasing α . In the limit of $\alpha = 1$, the results coincide with the conductance of s wave junctions in Fig. 4. The peak position can be explained by the expression of the Andreev reflection probability

$$|r^{he}|^2 = \frac{|t_N|^4}{|t_N|^4 + 4|r_N|^2 \cos^2(\theta + \phi_-)}, \quad (46)$$

$$\cos(\theta + \phi_-) = \frac{\sqrt{|\Delta|^2 - E^2}}{|\Delta|^2} \alpha \Delta_0 + \frac{E}{|\Delta|^2} \beta \Delta_{d_{xy}}, \quad (47)$$

$$\approx \frac{\sqrt{\Delta_0^2 - E^2}}{\Delta_0} \alpha + \frac{E}{\Delta_0} \beta \text{sgn}(k_x k_y). \quad (48)$$

In the last equation, we replace $\Delta_{d_{xy}}$ by $\Delta_{d_{\text{sign}}}$. The conductance peak (the resonance energy) is expected at an energy which satisfies $\cos(\theta + \phi_-) = 0$ as shown in Eq. (46). The resonance energies for $\alpha = 0$ and $\alpha = 1$ are $E = \Delta_0$ and $E = 0$, respectively. These resonance energies are independent of the wave numbers. Consequently the peak heights for $\alpha = 0$ and $\alpha = 1$ become unity. The peak heights for finite α , however, are always less than unity as shown in Fig. 5 because the resonance energy depends on wave numbers as shown in Eq. (47).

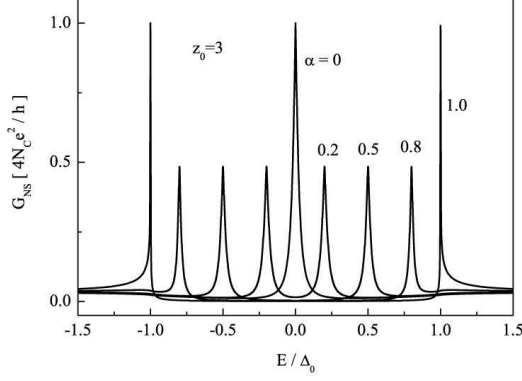


FIG. 5: The conductance is plotted as a function of E for $s + id_{xy}$ symmetry, where $z_0 = 3$.

The positions of the conductance peaks are roughly given by $E = \pm\alpha\Delta_0$, which can be understood by the resonance condition of $\cos(\theta + \phi_-) = 0$ in Eq. (48). Since the peak position is determined by α , relative amplitudes of s and d_{xy} components can be estimated from the peak splitting width observed in experiment. In the phenomenological theory, effects of the BTRSS on the conductance can be understood in terms of the shift of the resonance energy.

In theoretical studies, it is shown that the $s + id_{xy}$ wave BTRSS splits zero-energy peak of the local density of states^{54,62,63,64,65,66} and the ZBCP⁶⁷. Experimental results are, however, still controversial. Some experiments reported the split of the ZBCP at the zero magnetic field^{55,56,57,58,59}, other did not observe the splitting^{7,10,12,13,16,17,18}. Thus opinions are still divided among scientists on the BTRSS in high- T_c superconductors. If the BTRSS does not exist, we have to find another reasons for the peak splitting observed in experiments. In recent papers, we have showed that the interfacial randomness causes the split of the ZBCP in the zero magnetic field in both numerically⁷⁵ using the recursive Green function method^{76,77} and analytically⁷³ using the single-site approximation⁷⁸. Our conclusion, however, contradicts to those of a number of theories^{79,80,81,82,83,84} based on the quasiclassical Green function method^{85,86,87,88,89}. The drastic suppression of the

ZBCP by the interfacial randomness is the common conclusion of all the theories. The theories of the quasiclassical Green function method, however, concluded that the random potentials do not split the ZBCP.

V. EFFECTS OF MAGNETIC FIELD

The TRS is also broken by applying external magnetic fields onto NS junctions. The resonance at $E = 0$ is suppressed because a quasiparticle acquires a Aharonov-Bohm like phase from magnetic fields^{90,91,92}. Actually it is pointed out that the ZBCP in NS junctions splits into two peaks under the magnetic field^{54,55,68,69,70}. The re-

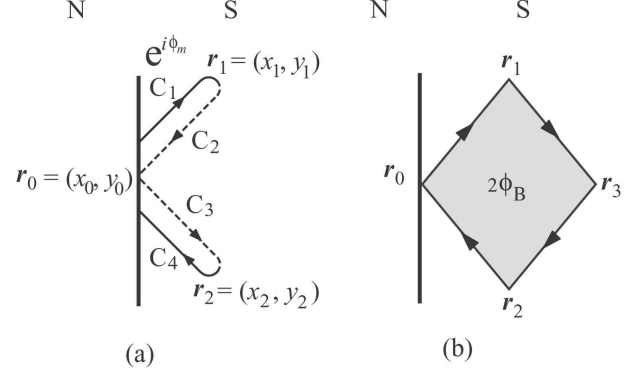


FIG. 6: The motion of a quasiparticle near the interface is illustrated.

flection process in Fig. 6(a) corresponds to A_s in Eq. (19). We consider uniform magnetic fields perpendicular to the xy plane (i.e., $B\hat{z}$) and assume the Landau gauge $\mathbf{A}_{ext} = Bx\hat{y}$. Effects of magnetic fields are taken into account through the phase of the wave function by using the gauge transformation. While traveling from \mathbf{r}_0 to \mathbf{r}_1 , an electronlike quasiparticle acquires a phase

$$e^{i\phi_m} = \exp \left[\frac{ie}{\hbar c} \int_{\mathbf{r}_0}^{\mathbf{r}_1} d\mathbf{l} \cdot \mathbf{A}_{ext}(\mathbf{l}) \right]. \quad (49)$$

Since the magnetic field is sufficiently weak, the integration path can be replaced by a straight line between \mathbf{r}_0 and \mathbf{r}_1 which is denoted by C_1 in Fig. 6(a),

$$\int_{\mathbf{r}_0}^{\mathbf{r}_1} d\mathbf{l} \cdot \mathbf{A}_{ext}(\mathbf{l}) = \frac{B}{2}(x_1 + x_0)(y_1 - y_0). \quad (50)$$

This approximation is justified when the radius of the cyclotron motion of a quasiparticle, $2\mu_F/(\hbar k_F mc)$, is much larger than ξ_0 . The condition is equivalent to the equation

$$\pi\Delta_0 \gg \hbar eB/mc. \quad (51)$$

In high- T_c materials, $\Delta_0 \sim 30\text{--}40$ meV, whereas $\hbar eB/mc$ is 10^{-1} meV for $B = 1$ Tesla, where we use the bare mass

of an electron. The phase shift on the way from \mathbf{r}_1 to \mathbf{r}_0 (C_2) in the hole branch is equal to $e^{i\phi_m}$. This is because the direction of a quasiparticle's motion and the sign of the charge on C_1 are opposite to those on C_2 at the same time. In the same way, we can show that the phase shifts on C_3 and C_4 in Fig. 6 (a) are also $e^{i\phi_m}$. Under the gauge transformation, the pair potential should be changed to

$$\Delta(\mathbf{r}, \mathbf{r}') \exp \left[\frac{ie}{\hbar c} \left(\int^{\mathbf{r}} + \int^{\mathbf{r}'} \right) d\mathbf{l} \cdot \mathbf{A}_{ext}(\mathbf{l}) \right]. \quad (52)$$

At \mathbf{r}_1 , a phase factor

$$\exp \left[\frac{-i2e}{\hbar c} \int^{\mathbf{r}_1} d\mathbf{l} \cdot \mathbf{A}_{ext}(\mathbf{l}) \right] \quad (53)$$

is multiplied to the Andreev reflection coefficients, where \mathbf{r} and \mathbf{r}' in Eq. (52) are set to be \mathbf{r}_1 . A phase factor

$$\exp \left[\frac{i2e}{\hbar c} \int^{\mathbf{r}_2} d\mathbf{l} \cdot \mathbf{A}_{ext}(\mathbf{l}) \right] \quad (54)$$

is also multiplied to the Andreev reflection coefficients at \mathbf{r}_2 . The total phase shift by the magnetic field along $C_1 \sim C_4$ in Fig. 6(a) ($e^{i2\phi_B}$) is then given by

$$\phi_B = 2\phi_m + \frac{e}{\hbar c} \int_{\mathbf{r}_1}^{\mathbf{r}_2} d\mathbf{l} \cdot \mathbf{A}_{ext}(\mathbf{l}), \quad (55)$$

$$= -\frac{eB}{\hbar c} (y_1 - y_0)(x_1 - x_0), \quad (56)$$

$$= -\frac{B}{B_0} \frac{k_y}{k_x}, \quad (57)$$

$$B_0 = \frac{\phi_0}{2\pi\xi_0^2}, \quad (58)$$

where $\phi_0 = 2\pi\hbar c/e$. On the way to Eq. (57), we use a relation

$$\left(\begin{array}{c} x_1 - x_0 \\ y_1 - y_0 \end{array} \right) // \left(\begin{array}{c} k_x \\ k_y \end{array} \right), \quad (59)$$

and $x_1 - x_0 \sim \xi_0$. We note that $2\phi_B$ is the gauge invariant magnetic flux passing through the gray area in Fig. 6(b), where $\mathbf{r}_3 = (2x_1 + x_0, y_0)$. Thus $2\phi_B$ remains unchanged in another gauges such as $\mathbf{A}_{ext} = -By\hat{\mathbf{x}}$ and penetrating magnetic fields $\mathbf{A}_{ext} = B\lambda_0 e^{-x/\lambda_0} \hat{\mathbf{y}}$ with $\lambda_0 \gg \xi_0$, where λ_0 is the penetration depth. In high- T_c materials, $\xi_0 \sim 2\text{nm}$ and $\lambda_0 \sim 200\text{nm}$.

Effects of magnetic field can be taken into account in the present theory by

$$A_s \rightarrow A_s e^{2i\phi_B}, \quad (60)$$

where A_s is defined in Eq. (19). We show the conductance in d_{xy} junctions calculated from Eqs. (21), (23), (25) and (60) in Fig. 7, where $z_0 = 3$ and 10 in (a) and (b), respectively. In high- T_c superconductors, B_0 is about 160 Tesla. The ZBCP decreases with increasing B in both (a) and (b). The degree of suppression due

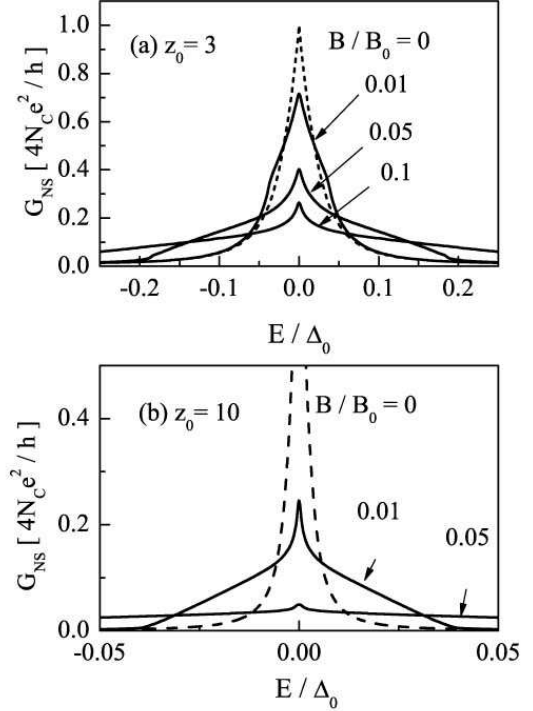


FIG. 7: The conductance under magnetic fields for d_{xy} symmetry, where $z_0 = 3$ and 10 in (a) and (b), respectively. In high- T_c material, B_0 is estimated to be 160 Tesla.

to magnetic fields depends on the transmission probability of the junction. More drastic suppression can be seen in lower transparent junctions. In (b), the ZBCP almost disappears for $B = 0.05B_0$. The ZBCP, however, remains one peak and does not split into two peaks even in the strong magnetic fields. The results in Fig. 7 are qualitatively well described by the analytical expression of the Andreev reflection probability for $E \ll \Delta_0$,

$$|r^{he}|^2 = \frac{|t_N|^4}{|t_N|^4 + 4|r_N|^2 \sin^2(\theta + \phi_B)}, \quad (61)$$

$$\simeq \frac{|t_N|^4 |\Delta|^2}{|t_N|^4 |\Delta|^2 + 4|r_N|^2 (E + |\Delta| \phi_B)^2}, \quad (62)$$

$$\sin(\theta + \phi_B) = \frac{E}{|\Delta|} \cos \phi_B + \frac{\sqrt{|\Delta|^2 - E^2}}{|\Delta|} \sin \phi_B. \quad (63)$$

Equation(63) implies that the resonance energy is shifted from $E = 0$ by magnetic fields because $\sin(\theta + \phi_B) = 0$ characterizes the resonance energy. We linearize the magnetic fields in $\sin(\theta + \phi_B)$ in Eq. (62). The results in Eq. (62) are similar to that in the argument of the Doppler shift in the quasiclassical approximation (QCA)⁵⁴. The supercurrents flows along the interface

shift the energy of a quasiparticle as

$$E \rightarrow E + \mathbf{v}_F \cdot \mathbf{p}_s, \quad (64)$$

$$\mathbf{p}_s = -\frac{e\mathbf{A}}{c} = \frac{eB\lambda_0}{c}e^{-x/\lambda_0}\hat{\mathbf{y}}, \quad (65)$$

where \mathbf{p}_s is the condensate momentum at the interface. In Eq. (65), d wave character of the supercurrent is not considered. The corresponding approximation in the present theory is replacing $E + |\Delta|\phi_B$ by $E + \Delta_0\phi_B$ in Eq. (62) and we find

$$|r^{he}|_{QCA}^2 = \frac{|t_N|^4|\Delta|^2}{|t_N|^4|\Delta|^2 + 4|r_N|^2(E + \Delta_0\phi_B)^2}. \quad (66)$$

In Fig. 7 (a), we show the conductance calculated from Eqs. (26) and (66) for $z_0 = 10$. In contrast to Fig. 7 (b), we find split of the ZBCP when magnetic fields are larger than the threshold magnetic field, B_c . The threshold depends on z_0 as shown in Fig. 8 (b), where B_c is plotted as a function of $1/z_0^2$ which is the normal transmission probability of junctions. The threshold decreases with decreasing $1/z_0^2$. This has been pointed out in the conductance calculated on the lattice model by using the QCA⁶⁹. In the lattice model, it was also shown that B_c decreases with the increase of the doping rate. The Fermi energy is a decreasing function of the doping rate. Therefore the transmission probability of junctions decreases with increasing the doping rate.

The phenomenological theory shows that the Aharonov-Bohm like phase from magnetic fields suppresses the resonance of the ZES and therefore decreases the ZBCP. The conductance expression similar to that in the QCA can be derived from the phenomenological theory. The ZBCP do not split under magnetic fields when we calculate the conductance using Eq. (62). When we neglect the d wave character of supercurrents, however, the peak splitting is found in the conductance of Eq. (66). Although Eqs. (62) and (66) are similar to each other, the response of the ZBCP to magnetic fields are qualitatively different. To make clear if a magnetic field splits the ZBCP or not, we need some numerical simulations, where effects of magnetic field are taken into account accurately. In experiments, some papers show the split of the ZBCP in magnetic fields^{55,57}. On the other hand, several papers report no splitting of the ZBCP^{16,93,94,95}.

We briefly discuss an important difference of the conductance in the present theory and that in the QCA. Here we assume that magnetic fields split the ZBCP and that Eq. (66) is valid. In Eq. (65), \mathbf{p}_s in the QCA is originally given by the vector potential, which is not an observable value. Thus the QCA does not satisfy the gauge invariance. This causes the remarkable difference in the threshold magnetic field. In the present theory, we consider uniform magnetic field and the normalization of magnetic fields (B_0) is about 160 Tesla. This value remains unchanged even if we consider penetrating magnetic field as $Be^{-x/\lambda_0}\hat{\mathbf{z}}$ with $\lambda_0 \gg \xi_0$. On the

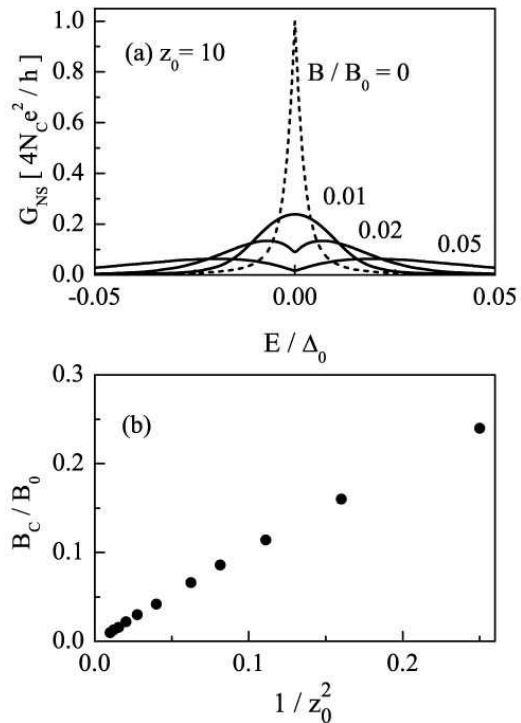


FIG. 8: The conductance in the quasiclassical approximation is plotted for several magnetic fields in (a), where $z_0 = 10$. In (b), critical magnetic fields are shown as a function of $1/z_0^2$.

other hand, the normalization for the penetrating magnetic fields in the QCA ($B_0^{QCA} = \phi_0/(2\pi\xi_0\lambda_0)$) is about 1.6 Tesla with $\lambda_0 \sim 100\xi_0$ ^{54,69}. For example in Fig. (8), we find that B_c is about $0.01B_0$ at $z_0 = 10$. Therefore B_c is estimated to be 1.6 Tesla in the present theory. The same results are interpreted as $B_c = 0.016$ Tesla if we use B_0^{QCA} in the QCA. The threshold magnetic field in the QCA is estimated to be much smaller than that in the present theory. Although the phenomenological theory reaches almost the same expression of the conductance as that in the QCA, two theories still lack a quantitative agreement in the threshold magnetic field. In experiments, the maximum value of magnetic fields, B_{max} , is about 10 Tesla^{16,93,94,95}. We may say that the split of the ZBCP cannot be observed in experiments if $B_c > B_{max}$ is satisfied.

VI. CONCLUSION

We have presented a phenomenological theory of the Andreev reflection to make clear reasons for the appearance of the zero-bias conductance peak (ZBCP) in normal-metal / d_{xy} wave superconductor junctions. Near

the junction interface, a quasiparticle suffers two kinds of reflection: (i) the normal reflection by the barrier potential at the NS interface and (ii) the Andreev reflection by the pair potential in the superconductor. The contribution of the two reflection processes to the transport coefficients are taken into account separately. The Andreev reflection coefficient are decomposed into a series expansion with respect to the normal reflection probability of NS junctions. Although the reflection coefficients are calculated in a phenomenological way, they coincide with the exact results. The expression of the Andreev reflection probability enables us to understand an importance of the unconventional pairing symmetry for the formation of the ZES. In addition to this, we easily understand that the ZES is a result of the interference effect of a quasiparticle. The phenomenological theory is applied to superconductors with a broken time-reversal symmetry state (BTRSS) and junctions under magnetic fields. The split of the ZBCP in $s + id_{xy}$ wave superconductors is understood in terms of the shift of the resonance energy by the s wave component. The Aharonov-Bohm like phase received from magnetic fields suppresses the degree of resonance of the ZES, which explains the suppression of the ZBCP in magnetic fields.

APPENDIX A: ANDREEV REFLECTION BY SPIN-TRIPLET SUPERCONDUCTORS

In the text, we consider two-dimensional spin-singlet superconductors and δ -function type potential barrier for simplicity. Here we generalize the phenomenological theory to spin-triplet superconductors in three-dimension. The pair potential in superconductors is given by

$$\hat{\Delta}(\mathbf{k}) = \begin{cases} i\mathbf{d}(\mathbf{k}) \cdot \hat{\boldsymbol{\sigma}}\hat{\sigma}_2 & : \text{triplet}, \\ i\mathbf{d}(\mathbf{k})\hat{\sigma}_2 & : \text{singlet}, \end{cases} \quad (\text{A1})$$

where $\hat{\sigma}_j$ for $j = 1, 2$ and 3 are Pauli matrices representing the spin degree of freedom. We assume that the current is in the x direction and consider a potential barrier

$$V(\mathbf{r}) = V_0 [\Theta(x) - \Theta(x - L)], \quad (\text{A2})$$

where L is the thickness of the insulating layer. The Andreev reflection coefficients in the absence of the insulator are calculated analytically

$$\hat{r}_{he} = -e^{-i\varphi_s} \hat{\Delta}_{(+)}^\dagger \hat{R}_{(+)}, \quad (\text{A3})$$

$$\hat{r}_{eh} = -e^{i\varphi_s} \hat{R}_{(-)} \hat{\Delta}_{(-)}^\dagger, \quad (\text{A4})$$

$$\hat{\Delta}_{(\pm)} = i\mathbf{d}_{\pm} \cdot \hat{\boldsymbol{\sigma}}\hat{\sigma}_2, \quad (\text{A5})$$

$$\hat{R}_{(\pm)} = \frac{1}{2|\mathbf{q}_{\pm}|} \sum_{l=1}^2 \left[\frac{K_{l,\pm}}{\Delta_{l,\pm}^2} \hat{P}_{l,\pm} \right], \quad (\text{A6})$$

$$\Delta_{l,\pm} = \sqrt{|\mathbf{d}_{\pm}|^2 - (-1)^l |\mathbf{q}_{\pm}|}, \quad (\text{A7})$$

$$K_{l,\pm} = \sqrt{E^2 - \Delta_{l,\pm}^2} - E, \quad (\text{A8})$$

$$\hat{P}_{l,\pm} = |\mathbf{q}_{\pm}| \hat{\sigma}_0 - (-1)^l \mathbf{q}_{\pm} \cdot \hat{\boldsymbol{\sigma}}, \quad (\text{A9})$$

$$\mathbf{q}_{\pm} = i\mathbf{d}_{\pm} \times \mathbf{d}_{\pm}^*, \quad (\text{A10})$$

$$\mathbf{d}_{\pm} = \mathbf{d}(\pm k_x, k_y, k_z), \quad (\text{A11})$$

where φ_s is a macroscopic phase of superconductor, $l (= 1 \text{ or } 2)$ indicates the two spin branches of Cooper pairs and $\hat{\sigma}_0$ is the 2×2 unit matrix. The normal transmission and the normal reflection coefficients of the insulator are calculated as

$$\hat{t}_N = \frac{-2i\bar{k}_x \bar{p}_x e^{-ik_x L}}{z_1^*} \hat{\sigma}_0, \quad (\text{A12})$$

$$\hat{r}_N = \frac{-z_0}{z_1^*} \hat{\sigma}_0, \quad (\text{A13})$$

$$z_0 = \frac{V_0}{\mu_F} \sinh(p_x L), \quad (\text{A14})$$

$$z_1 = (\bar{p}_x^2 - \bar{k}_x^2) \sinh(p_x L) + 2i\bar{k}_x \bar{p}_x \cosh(p_x L), \quad (\text{A15})$$

where $p_x = \sqrt{(V_0/\mu_F) - (k_x/k_F)^2}$ is the wave number at the insulator and $\bar{p}_x = p_x/k_F$.

The argument in Sec. II leads to the exact expression of the Andreev and the normal reflection coefficients⁹⁶ which are given by

$$\hat{r}_{ee} = -z_0 z_1 [\hat{\sigma}_0 - \hat{W}] \left[|z_1|^2 \hat{\sigma}_0 - z_0^2 \hat{W} \right]^{-1}, \quad (\text{A16})$$

$$\hat{r}_{he} = -e^{-i\varphi_s} 4\bar{k}_x^2 \bar{p}_x^2 \hat{\Delta}_{(+)}^\dagger \hat{R}_{(+)} \left[|z_1|^2 \hat{\sigma}_0 - z_0^2 \hat{W} \right]^{-1}, \quad (\text{A17})$$

$$\hat{W} = \hat{R}_{(-)} \hat{\Delta}_{(-)}^\dagger \hat{\Delta}_{(+)} \hat{R}_{(+)}. \quad (\text{A18})$$

The results of unitary states including the spin-singlet states can be obtained when we use following relations

$$\hat{R}_{(\pm)} = \frac{\sqrt{E^2 - |D_{\pm}|^2} - E}{|D_{\pm}|^2} \hat{\sigma}_0, \quad (\text{A19})$$

$$|D_{\pm}| = \begin{cases} |d_{\pm}| & : \text{singlet} \\ |\mathbf{d}_{\pm}| & : \text{triplet}, \end{cases} \quad (\text{A20})$$

in Eqs. (A16)-(A18). In spin-singlet superconductors, we show that the internal phase of a Cooper pair is responsible for the ZES. In spin-triplet superconductors, the internal spin degree of freedom of a Cooper pair has another possibilities for the formation of some surface states in subgap energies.

-
- * Electronic address: asano@eng.hokudai.ac.jp
- ¹ C. C. Tsuei and J. R. Kirtley, *Rev. Mod. Phys.* **72**, 969 (2000).
 - ² M. Sigrist and T. M. Rice, *J. Phys. Soc. Jpn.* **61**, 4283 (1992); *Rev. Mod. Phys.* **67**, 503 (1995).
 - ³ D. A. Wollman, D. J. Van Harlingen, W. C. Lee, D. M. Ginsberg, and A. J. Leggett, *Phys. Rev. Lett.* **71**, 2134 (1993).
 - ⁴ M. A. Tanatar, S. Nagai, Z. Q. Mao, Y. Maeno, and T. Ishiguro, *Phys. Rev. B* **63**, 064505 (2001); M. A. Tanatar, M. Suzuki, S. Nagai, Z. Q. Mao, Y. Maeno, and T. Ishiguro, *Phys. Rev. Lett.* **86**, 2649 (2001).
 - ⁵ K. Izawa, H. Takahashi, H. Yamaguchi, Y. Matsuda, M. Suzuki, T. Sasaki, T. Fukase, Y. Yoshida, R. Settai, and Y. Onuki *Phys. Rev. Lett.* **86**, 2653 (2001); K. Izawa, H. Yamaguchi, T. Sasaki, and Y. Matsuda, *Phys. Rev. Lett.* **88**, 027002 (2002).
 - ⁶ Y. Tanaka and S. Kashiwaya, *Phys. Rev. Lett.* **74**, 3451 (1995).
 - ⁷ S. Kashiwaya and Y. Tanaka, *Rep. Prog. Phys.* **63**, 1641 (2001).
 - ⁸ T. Löfwander, V. S. Shumeiko, and G. Wendin, *Supercond. Sci. Technol.* **14**, R53 (2001).
 - ⁹ S. Kashiwaya, Y. Tanaka, M. Koyanagi, H. Takashima, and K. Kajimura, *Phys. Rev. B* **51**, 1350 (1995).
 - ¹⁰ L. Alff, H. Takashima, S. Kashiwaya, N. Terada, H. Ihara, Y. Tanaka, M. Koyanagi, and K. Kajimura, *Phys. Rev. B* **55**, 14757 (1997).
 - ¹¹ W. Wang, M. Yamazaki, K. Lee, and I. Iguchi, *Phys. Rev. B* **60**, 4272 (1999).
 - ¹² J. Y. T. Wei, N. -C. Yeh, D. F. Garrigus, and M. Strasik, *Phys. Rev. Lett.* **81**, (1998) 2542.
 - ¹³ I. Iguchi, W. Wang, M. Yamazaki, Y. Tanaka, and S. Kashiwaya, *Phys. Rev. B* **62**, R6131 (2000).
 - ¹⁴ J. Geerk, X. X. Xi, and G. Linker, *Z. Phys. B* **73**, 329 (1988).
 - ¹⁵ Z. Q. Mao, M. M. Rosario, K. D. Nelson, K. Wu, I. G. Deac, P. Schiffer, Y. Liu, T. He, K. A. Regan, and R. J. Cava, *Phys. Rev. B* **67**, 094502 (2003).
 - ¹⁶ J. W. Ekin, Y. Xu, S. Mao, T. Venkatesan, D. W. Face, M. Eddy, and S. A. Wolf, *Phys. Rev. B* **56**, 13746 (1997).
 - ¹⁷ A. Sawa, S. Kashiwaya, H. Obara, H. Yamasaki, M. Koyanagi, Y. Tanaka, and N. Yoshida, *Physica C* **339**, 107 (2000).
 - ¹⁸ H. Aubin, L. H. Greene, S. Jian, and D. G. Hinks, *Phys. Rev. Lett.* **89**, 177001 (2002).
 - ¹⁹ C. R. Hu, *Phys. Rev. Lett.* **72**, 1526 (1994).
 - ²⁰ Y. S. Barash, H. Burkhardt, and D. Rainer, *Phys. Rev. Lett.* **77**, 4070 (1996).
 - ²¹ Y. Tanaka and S. Kashiwaya, *Phys. Rev. B* **53**, R11957 (1996).
 - ²² Y. Tanaka and S. Kashiwaya, *Phys. Rev. B* **56**, 892 (1997).
 - ²³ Y. Tanaka and S. Kashiwaya, *Phys. Rev. B* **58**, R2948 (1998).
 - ²⁴ Y. Asano, *Phys. Rev. B* **64**, 224515 (2001).
 - ²⁵ Y. Asano, *Phys. Rev. B* **64**, 014511 (2001).
 - ²⁶ L. J. Buchholtz and G. Zwicknagl, *Phys. Rev. B* **23**, 5788 (1981).
 - ²⁷ Y. Asano, *J. Phys. Soc. Jpn.* **71**, 905 (2002).
 - ²⁸ M. Yamashiro, Y. Tanaka, and S. Kashiwaya, *Phys. Rev. B* **56**, 7847 (1997).
 - ²⁹ M. Yamashiro, Y. Tanaka, Y. Tanuma, and S. Kashiwaya, *J. Phys. Soc. Jpn.* **67**, 3224 (1998).
 - ³⁰ M. Yamashiro, Y. Tanaka, N. Yoshida, and S. Kashiwaya, *J. Phys. Soc. Jpn.* **68**, 2019 (1999).
 - ³¹ J. -X. Zhu, B. Friedman, and C. S. Ting, *Phys. Rev. B* **59**, 9558 (1999).
 - ³² S. Kashiwaya, Y. Tanaka, N. Yoshida, and M. R. Beasley, *Phys. Rev. B* **60**, 3572 (1999).
 - ³³ I. Žutić and O. T. Valls, *Phys. Rev. B* **60**, 6320 (1999).
 - ³⁴ N. Yoshida, Y. Tanaka, J. Inoue, and S. Kashiwaya, *J. Phys. Soc. Jpn.* **68**, 1071 (1999).
 - ³⁵ N. Yoshida, Y. Asano, H. Itoh, Y. Tanaka, and J. Inoue, *J. Phys. Soc. Jpn.* **72**, 895 (2003).
 - ³⁶ T. Hirai, N. Yoshida, Y. Tanaka, J. Inoue, and S. Kashiwaya, *J. Phys. Soc. Jpn.* **70**, 1885 (2001).
 - ³⁷ T. Hirai, Y. Tanaka, N. Yoshida, Y. Asano, J. Inoue, and S. Kashiwaya, *Phys. Rev. B* **67**, 174501 (2003).
 - ³⁸ Y. Tanaka and S. Kashiwaya, *J. Phys. Soc. Jpn.* **68**, 3485 (1999); *J. Phys. Soc. Jpn.* **69**, 1152 (2000).
 - ³⁹ Y. Tanaka, Yu. V. Nazarov, and S. Kashiwaya, *Phys. Rev. Lett.* **90**, 167003 (2003).
 - ⁴⁰ Y. Tanuma, K. Kuroki, Y. Tanaka, and S. Kashiwaya, *Phys. Rev. B* **64**, 214510 (2001).
 - ⁴¹ Y. Tanuma, K. Kuroki, Y. Tanaka, R. Arita, S. Kashiwaya, and H. Aoki, *Phys. Rev. B* **66**, 094507 (2002).
 - ⁴² Y. Tanaka, T. Hirai, K. Kusakabe, and S. Kashiwaya, *Phys. Rev. B* **60**, 6308 (1999).
 - ⁴³ C. Honerkamp and M. Sigrist, *J. Low. Temp. Phys.* **111**, 898 (1998); *Prog. Theor. Phys.* **100**, 53 (1998).
 - ⁴⁴ N. Stefanakis, *Phys. Rev. B* **64**, 224502 (2001); *J. Phys. Cond. Matt.* **13**, 3643 (2001).
 - ⁴⁵ K. Sengupta, I. Žutić, H.-J. Kwon, V. M. Yakovenko, and S. Das Sarma, *Phys. Rev. B* **63**, 144531 (2001).
 - ⁴⁶ Y. Asano and K. Katabuchi, *J. Phys. Soc. Jpn.* **71**, 1974 (2002).
 - ⁴⁷ Y. Asano, Y. Tanaka, M. Sigrist, and S. Kashiwaya, *Phys. Rev. B* **67**, 184505 (2003).
 - ⁴⁸ Y. Tanaka and S. Kashiwaya, *Phys. Rev. B* **53**, 9371 (1996).
 - ⁴⁹ M. Matsumoto and H. Shiba, *J. Phys. Soc. Jpn.* **64**, 1703 (1995).
 - ⁵⁰ S. Shirai, H. Tsuchiura, Y. Asano, Y. Tanaka, J. Inoue, Y. Tanuma, and S. Kashiwaya, *J. Phys. Soc. Jpn.* **72**, No.9 (2003) in press.
 - ⁵¹ A. F. Andreev, *Zh. Eksp. Theor. Fiz.* **46**, 1823 (1964) [*Sov. Phys. JETP* **19**, 1228 (1964)].
 - ⁵² P. G. de Gennes, *Superconductivity of Metals and Alloys*, (Benjamin, New York, 1966).
 - ⁵³ Y. Tanaka and S. Kashiwaya, *Physica C* **352**, 30 (2001).
 - ⁵⁴ M. Fogelström, D. Rainer, and J. A. Sauls, *Phys. Rev. Lett.* **79**, 281 (1997).
 - ⁵⁵ M. Covington, M. Aprili, E. Paraoanu, L. H. Greene, F. Xu, J. Zhu, and C. A. Mirkin, *Phys. Rev. Lett.* **79**, 277 (1997).
 - ⁵⁶ A. Biswas, P. Fournier, M. M. Qazilbash, V. N. Smolyaninova, H. Balci, and R. L. Greene, *Phys. Rev. Lett.* **88**, 207004 (2002).
 - ⁵⁷ Y. Dagan and G. Deutscher, *Phys. Rev. Lett.* **87**, 177004 (2001).
 - ⁵⁸ A. Sharoni, O. Millo, A. Kohen, Y. Dagan, R. Beck, G. Deutscher, and G. Koren, *Phys. Rev. B* **65**, 134526 (2002).

- (2002).
- ⁵⁹ A. Kohen, G. Leibovitch, and G. Deutscher, Phys. Rev. Lett. **90**, 207005 (2003).
 - ⁶⁰ M. Matsumoto and H. Shiba, J. Phys. Soc. Jpn. **64**, 4867 (1995).
 - ⁶¹ R. B. Laughlin, Phys. Rev. Lett. **80**, 5188 (1998).
 - ⁶² S. Kashiwaya, Y. Tanaka, M. Koyanagi, and K. Kjimura, J. Phys. Chem. Solids **56**, 1721 (1995).
 - ⁶³ Y. Tanuma, Y. Tanaka, M. Ogata, and S. Kashiwaya, J. Phys. Soc. Jpn. **67**, 1118 (1998).
 - ⁶⁴ Y. Tanuma, Y. Tanaka, M. Ogata, and S. Kashiwaya, Phys. Rev. B **60**, 9817 (1999).
 - ⁶⁵ Y. Tanuma, Y. Tanaka, and S. Kashiwaya, Phys. Rev. B **64**, 214519 (2001).
 - ⁶⁶ I. Lubimova and G. Koren, cond-mat/0306030.
 - ⁶⁷ N. Kitaura, H. Itoh, Y. Asano, Y. Tanaka, J. Inoue, Y. Tanuma, and S. Kashiwaya, J. Phys. Soc. Jpn. **72**, (2003) in press.
 - ⁶⁸ Y. Tanaka, H. Tsuchiura, Y. Tanuma, and S. Kashiwaya, J. Phys. Soc. Jpn. **71**, 271 (2002).
 - ⁶⁹ Y. Tanaka, H. Itoh, H. Tsuchiura, Y. Tanuma, J. Inoue, and S. Kashiwaya, J. Phys. Soc. Jpn. **71**, 2005 (2002).
 - ⁷⁰ Y. Tanaka, Y. Tanuma, K. Kuroki, and S. Kashiwaya, J. Phys. Soc. Jpn. **71**, 2102 (2002).
 - ⁷¹ G. E. Blonder, M. Tinkham, and T. M. Klapwijk, Phys. Rev. B **25**, 4515 (1982).
 - ⁷² Y. Takane and H. Ebisawa, J. Phys. Soc. Jpn. **61**, 1685 (1992).
 - ⁷³ Y. Asano, Y. Tanaka, and S. Kashiwaya, cond-mat/0302287.
 - ⁷⁴ Y. Tanaka, T. Asai, N. Yoshida, J. Inoue, and S. Kashiwaya, Phys. Rev. B **61**, R11902 (2000).
 - ⁷⁵ Y. Asano and Y. Tanaka, Phys. Rev. B **65**, 064522 (2002); "Toward the controllable Quantum State" Eds. H. Takayanagi and J. Nitta, 185, (World Scientific, Singapore, 2003).
 - ⁷⁶ P. A. Lee and D. S. Fisher, Phys. Rev. Lett. **47**, 882 (1981).
 - ⁷⁷ Y. Asano, Phys. Rev. B **63**, 052512 (2001).
 - ⁷⁸ Y. Asano and G. E. W. Bauer, Phys. Rev. B **54**, 11602 (1996); Erratum **54**, 9972 (1997).
 - ⁷⁹ Y. S. Barash, A. A. Svidzinsky, and H. Burkhardt, Phys. Rev. B **55**, 15282 (1997).
 - ⁸⁰ A. A. Golubov, M. Y. Kupriyanov, Pis'ma Zh. Eksp. Teor. fiz **69**, 242 (1999). [Sov. Phys. JETP Lett. **69**, 262 (1999).]; **67**, 478 (1998). [Sov. Phys. JETP Lett. **67**, 501 (1998).]
 - ⁸¹ A. Poenicke, Yu. S. Barash, C. Bruder, and V. Istyukov, Phys. Rev. B **59**, 7102 (1999).
 - ⁸² K. Yamada, Y. Nagato, S. Higashitani, and K. Nagai, J. Phys. Soc. Jpn. **65**, 1540 (1996).
 - ⁸³ Y. Tanaka, Y. Tanuma, and S. Kashiwaya, Phys. Rev. B **64**, 054510 (2001).
 - ⁸⁴ T. Lück, U. Eckern, and A. Shelankov, Phys. Rev. B **63**, 064510 (2001).
 - ⁸⁵ G. Eilenberger, Z. Phys. **214**, 195 (1968).
 - ⁸⁶ A. I. Larkin and Yu. N. Ovchinnikov, Eksp. Teor. Fiz. **55**, 2262 (1986). [Sov. Phys. JETP **28**, 1200 (1968).]
 - ⁸⁷ A. V. Zaitsev, Zh. Eksp. Teor. Fiz. **86**, 1742 (1984). [Sov. Phys. JETP **59**, 1015 (1984).]
 - ⁸⁸ A. L. Schelankov, J. Low. Tem. Phys. **60**, 29 (1985).
 - ⁸⁹ C. Bruder, Phys. Rev. B **41**, 4017 (1990).
 - ⁹⁰ Y. Asano, Phys. Rev. B **61**, 1732 (2000).
 - ⁹¹ Y. Asano and T. Kato, J. Phys. Soc. Jpn. **69**, 1125 (2000).
 - ⁹² Y. Asano and T. Yuito, Phys. Rev. B **62**, 7477 (2000).
 - ⁹³ M. M. Qazilbash, A. Biswas, Y. Dagan, R. A. Ott, and R. L. Greene, Phys. Rev. B **68**, 024502 (2003).
 - ⁹⁴ L. Alff, S. Kleefishch, U. Schoop, M. Zittartz, T. Kemen, T. A. Marx, and R. Gross, Eur. Phys. J. B **5**, 423 (1998).
 - ⁹⁵ A. Sawa, S. Kashiwaya, H. Kashiwaya, H. Obara, H. Yamasaki, M. Koyanagi, I. Kurosawa, and Y. Tanaka, Physica C **357-360**, 294 (2001).
 - ⁹⁶ Y. Asano, Y. Tanaka, Y. Matsuda, and S. Kashiwaya, cond-mat/0306155.